Al-Khwarizmi Engineering Journal, Vol. 7, No. 1, PP 82 - 94 (2011)

Al-Khwarizmi Engineering Journal

A Digital-Based Optimal AVR Design of Synchronous Generator Exciter Using LQR Technique

Ibraheem Kasim Ibraheem

Department of Computer Engineering/ College of Engineering/ University of Baghdad

Email: ibraheem151@gmail.com

(Received 18 April 2010; Accepted 23 December 2010)

Abstract

In this paper a new structure for the AVR of the power system exciter is proposed and designed using digital-based LQR. With two weighting matrices R and Q, this method produces an optimal regulator that is used to generate the feedback control law. These matrices are called state and control weighting matrices and are used to balance between the relative importance of the input and the states in the cost function that is being optimized. A sample power system composed of single machine connected to an infinite- bus bar (SMIB) with both a conventional and a proposed Digital AVR (DAVR) is simulated. Evaluation results show that the DAVR damps well the oscillations of the terminal voltage and presents a faster response than that of the conventional AVR.

Keywords: *Exciter design, AVR, LQR, state-feedback, SMIB.*

1. Introduction

Excitation control of generators is a very important topic in the field of power systems. A good excitation control, indeed, has proven to be very efficient to support the voltage on the power system, to enhance its transient stability and to damp its oscillations [1].

The basic requirement is that the excitation system supply and automatically adjust the field current of the synchronous generators to maintain the terminal voltage as the output varies within the continuous capability of the generator (Generator considerations), while the excitation system should contribute to effective control of voltage and enhancement of system stability (Power syste*m considerations*) [2].

With the emergence of digital technology, digital based excitation systems are being evolved and this development has added to the AC and ST types of excitation control systems [3]. Recent trend in modern excitation control systems is towards the use of the digital electronics to perform control and protection functions [4].

Many features are available in digital excitation in comparison to analog excitation systems: greater precision, immunity to component variations, reduced cost, reduced hardware and hence less maintenance cost, availability of on board test features, implement ability of fuzzy and adaptive or other control schemes. Microprocessors or microcontroller or PCs used in these systems give capability to provide much more information and greater control. Flexible software or using different software with the same unit provides greater choice, possibility of more protection features, greater memory and self monitoring of PC cards [4]. In addition, this type of solution is much cheaper than heavy equipments like FACTS (Flexible Alternating Current Transmission System) which are necessary only in very specific cases, as far as oscillation damping is concerned.

Digital systems are the state of the art systems, both for new synchronous machines as well as for modernizing existing older plants. Now with digital control, the excitation system models are modified to include proportional gain K_P and integral gain K_I which are adjustable [4].

Studies on the detailed models of digital excitation systems with SMIB have not been

reported well in the literature and, hence, they have drawn much attention. Many attempts have been done in the last years regarding the design of excitation control systems. The H∞ control theory has been exploited in [5] to design an excitation control system using LMI (Linear Matrix Inequality) to damp power system oscillations and control of terminal voltage simultaneously; weighting filters have to be designed for this technique. The authors in [6] designed a neurocontroller to replace both the conventional automatic voltage regulator (AVR) and the turbine governor of the power systems, while in [7] a separate neurocontroller for the each of the AVR and the turbine governor has been designed. In [8] researchers present a step-by-step design methodology of an adaptive neuro-fuzzy inference system (ANFIS) based AVR and power system stabilizer (PSS) and also demonstrated its performance in a single-machine-infinite-bus and a multi-machine power system through digital simulation. In [9], an adaptive design of an automatic voltage regulator (AVR) control scheme for synchronous generators is introduced in the presence of unknown variations of the power system operating conditions; the AVR design is based on pole-assignment technique and the estimation is performed by kalman filter. While in [10], an efficient and powerful design method suitable for calculating optimal proportional-integral-derivative (PID) controllers for AVR systems is proposed. The method is an improved version of the Discrete Action Reinforcement Learning Automata (DARLA). In [11], authors employed a loop-shaping method, which is achieved via a parameter space approach accomplished by symbolic method called quantifier elimination (QE) and apply it to design PI control type AVR of the excitation control. In [12], a step-by-step coordinated design procedure for power system stabilizers (PSSs) and automatic voltage regulators (AVRs) in a strongly coupled system is described.

Figure 1 shows a typical continuous feedback control system. Almost all of the continuous controllers can be built using analog electronics [13, 14].

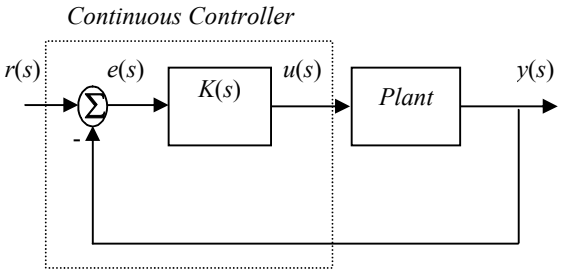

Fig. 1. Analog Closed-Loop Control System.

The continuous controller, enclosed in the dashed square, can be replaced by a digital controller, as shown in figure 2 below, that performs the same control task as the continuous controller. The basic difference between these two controllers is that the digital system operates on discrete signals (or samples of the sensed signal) rather than on continuous signals [13,14].

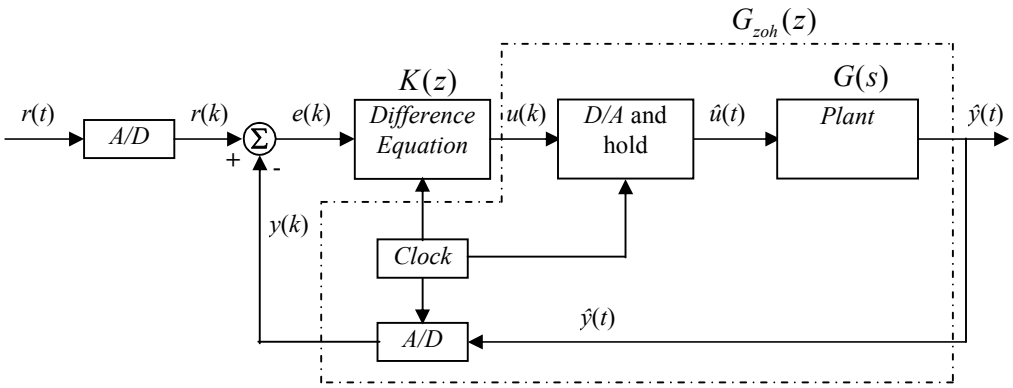

Fig. 2. Closed-loop Control System.

In the above schematic drawing of the digital control system, it can be seen that the digital control system contains both discrete and continuous portions.

The clock connected to the D/A and A/D converters supplies a pulse every T_s second and each D/A and A/D sends a signal only when the pulse arrives. The purpose of having this pulse is to require that $G_{zoh}(z)$ have only samples of $u(k)$ to work on and produce only samples of output $y(k)$; thus, $G_{zoh}(z)$ can be realized as a discrete function [14].

Now the schematic will be drawn by placing $G_{zoh}(z)$ in place of the continuous portion. By placing $G_{zoh}(z)$, a digital control system $K(z)$ can be designed which deals only with discrete functions, see figure 3. When designing a digital control system, the discrete equivalent (discrete-state-space or transfer function system) of the continuous portion must be found so that only discrete functions are dealt with in this work [14]. That will be done in the next section.

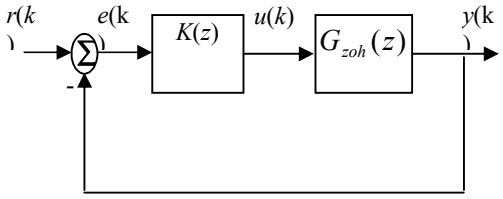

Fig. 3. Closed-Loop Digital Control System.

This paper is organized as follows: a brief introduction to the digital design of linear quadratic regulator is given in section 2; section 3 describes the state-space modeling of the power system excitation control. Evaluation results are included in section 4. Finally conclusions are given in section 5.

2. Digital Control System Design with Optimal Linear Quadratic Regulator

Given an analog linear system with state-space equation:

$$\dot{x}(t) = \mathrm{A}\,\mathrm{x}(t) + \mathrm{B}\,\mathrm{u}(t)$$
$$y(t) = \mathrm{C}\,\mathrm{x}(t) + \mathrm{D}\,\mathrm{u}(t) \qquad \ldots(1)$$

where $x(t)$ is an $n \times 1$ real vector, $u(t)$ is an $m \times 1$ real vector, and $y(t)$ is an $l \times 1$ real vector, the matrices in the equations are:

$A = n \times n$ state matrix.
$B = n \times m$ input or control matrix.
$C = l \times n$ output matrix.
$D = l \times m$ direct transmission matrix.

With piecewise constant inputs over a given sampling period (T_s), the system state variables at the end of each period can be related by a difference equation. It is obtained by examining the solution of the analog state (eq. (1)) over T_s [15,16].

The discrete –time state equation is given by [15,16]:

$$x(k+1) = A_d\, x(k) + B_d\, u(k) \qquad \ldots(2)$$

Where

$$A_d = e^{AT_s} \qquad \ldots(3)$$

$$B_d = \int_0^{T_s} e^{A\lambda} B\, d\lambda \qquad \ldots(4)$$

The output equation evaluated at time kT_s is [15,16]:

$$y(k) = C\, x(k) + D\, u(k) \qquad \ldots(5)$$

The discrete-time state-space representation is given by eq(2) and eq(5). It should be noted that the matrices C_d & D_d of the discrete system are equal to its corresponding matrices of the continuous system.

One of the difficulties in designing the pole placement controllers is the selection of closed-loop pole locations, especially in a large dimensional state space system. An alternative approach is to use an optimization based strategy to design the controller. Minimization of the square of an error for a linear system results in a *Linear Quadratic Regulator* abbreviated as *LQR* [16, 17]. The schematic of a full-state feedback system is drawn in figure 4.

The next step is to assume that all states are measurable, and find the control matrix (K). The LQR method will be used to find the control matrix (K).

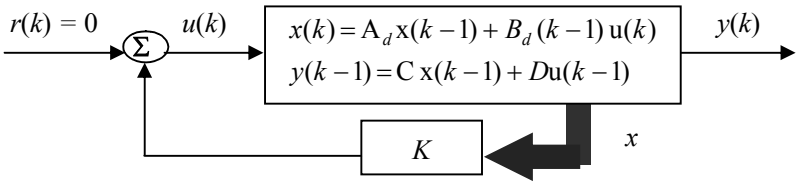

Fig. 4. Quadratic Optimal Control System.

The LQR design approach involves the minimization of a weighted sum of quadratic functions of the state and the control effort. If a quadratic function of only the states is minimized, the control effort could become unbounded. To overcome these difficulties, the quadratic function of the control effort is minimized as well [15].

Consider the discrete-time state-space system:

$$x(k+1) = A_d\, x(k) + B_d\, u(k) \quad \ldots(6)$$

$$y(k) = C\, x(k) + D\, u(k) \quad \ldots(7)$$

A control law $u(k) = -K * x(k)$ has to be found so that a cost function [15,16]:

$$J = \frac{1}{2}\sum_{0}^{\infty}[x^T(k)\, Q\, x(k) + u^T(k)\, R\, u(k)] \quad \ldots(8)$$

is minimized, where Q and R are constant symmetric state and control weighting matrices to be selected by the designer, with Q positive semidefinite and R positive definite. When the objective function is a sum of an infinite number of terms, known as the *infinite horizon problem*, the steady state solution is the optimal solution [16, 18].

As some of the states may be allowed to be zero and all control efforts have a cost associated with them, some conditions must be satisfied [16,18]:

1. $x^T Q\, x \geq 0 \;\; \forall\, x$. …(9)
2. $u^T R\, u \geq 0 \;\; \forall\, x \neq 0$. …(10)
3. The (A_d, B_d) is controllable (stablizable).
4. The pair (A_d, C) is observable (detectable).

The state weighting matrix can be decomposed as follows [16]:

$$Q = C^T C \quad \ldots(11)$$

where C is the output matrix and is positive definite for Q positive definite and positive semidefinite for Q positive semidefinite. Conditions (3) and (4) guarantee the Riccati equation does not diverge and a steady-state condition is reached. The resulting algebraic Riccate equation is in the form [16, 18, 19]:

$$S = A_d^T[S - SB_d(B_d^T SB_d + R^{-1})B_d^T S]A_d + Q \quad \ldots(12)$$

It is called Discrete Algebraic Riccate Equation (DARE), and it has a unique positive definite solution. However, the equation is clearly difficult to solve in general and is typically solved numerically [19].

The optimal state feedback control law corresponding to the steady-state regulator is [15,16, 18, 20]:

$$u(k) = -K\, x(k) \quad \ldots(13)$$

$$K = [R + B_d^T SB_d]^{-1} B_d^T SA \quad \ldots(14)$$

Notice that this optimal control law K can be calculated once and for all at the very beginning.

Unlike other design methods, the full-state feedback system does not compare the output to the reference; instead, it compares all states multiplied by the control matrix $(K * x)$ to the reference (see Figure.4). Thus, it is not expected to see the output equals the input. To obtain the desired output, the reference input should be scaled so that the output equals the reference. This can be easily done by introducing a feedforward scaling factor called *Nbar*. The basic schematic with Nbar is shown in figure 5 [14, 20].

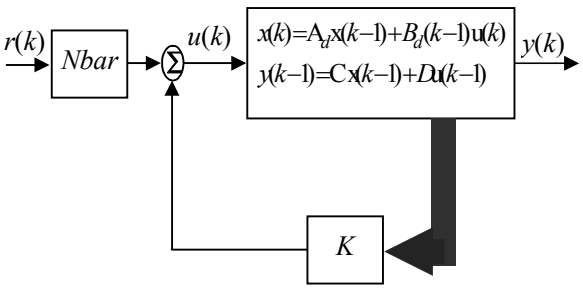

Fig. 5. Quadratic Optimal Control System.

The scaling factor *Nbar* can be calculated as follows [15,20]:

$$\overline{N} = N_u + K\,N_x \qquad \ldots(15)$$

Where

$$\begin{bmatrix} N_x \\ N_u \end{bmatrix} = \begin{bmatrix} A_d - I & B_d \\ C & 0 \end{bmatrix}^{-1} \cdot \begin{bmatrix} 0 \\ I \end{bmatrix} \qquad \ldots(16)$$

Finally, it is important to present general guidelines for choosing the state and control weighting matrices Q and R [15,20]:

1. Both of them must be symmetric with Q that is positive semidefinite and R that is positive definite.
2. R is usually chosen to be purely diagonal matrix while Q is given by eq (11).
3. It is a normal practice to select initial values for Q and R, carry out the *design* of the feedback gain matrix K, and then simulate the resulting system and view the response. Values of Q and R are changed as required by the designer and the procedure is repeated.

3. Modeling of the Power Plant Exciter System.

The excitation control system is one of the important factors in the transient study of power system analysis. It controls the generated EMF of the generator and therefore controls not only the output voltage but the power factor and the current magnitude as well. A typical relationship between the excitation control system and the generator is illustrated in figure 6 [21].

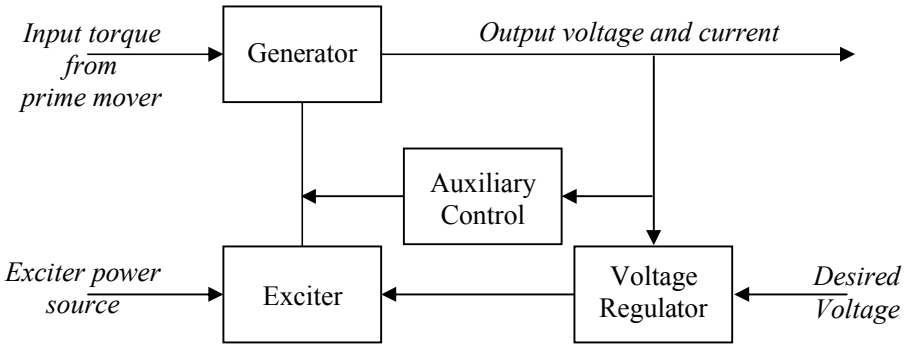

Fig. 6. Typical Arrangement of Excitation Components.

The exciter provides a dc power to the synchronous machine field winding, constituting the power stage of the excitation system. While the regulator process and amplifies input control signals to a level and forms appropriate control of the exciter. The other protective and limiting functions are achieved by auxiliary control [2].

The power system considered in this study is modeled as a synchronous generator connected to an infinite bus bar. A static excitation system and automatic voltage regulator (AVR) are employed to maintain the terminal voltage profile as shown in figure 7 [22,23].

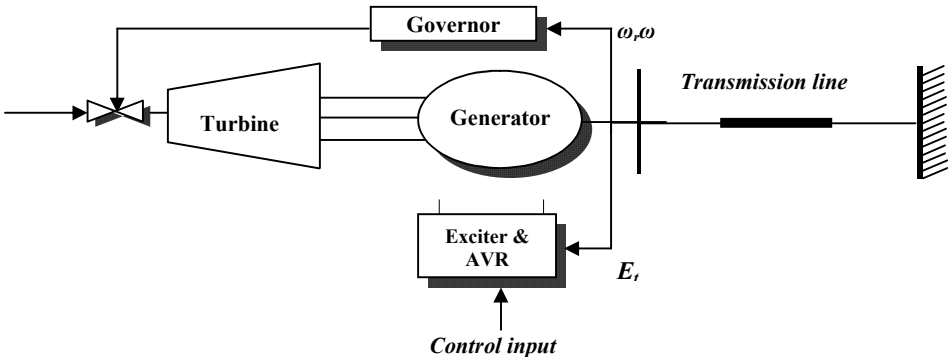

Fig. 7. Power System Configuration.

The block diagram of the linearized exciter model with the conventional AVR is shown in figure 8 [2, 4, 22, 23]: Where the parameters of this linearized model are defined in Table 1 [1,2,24].

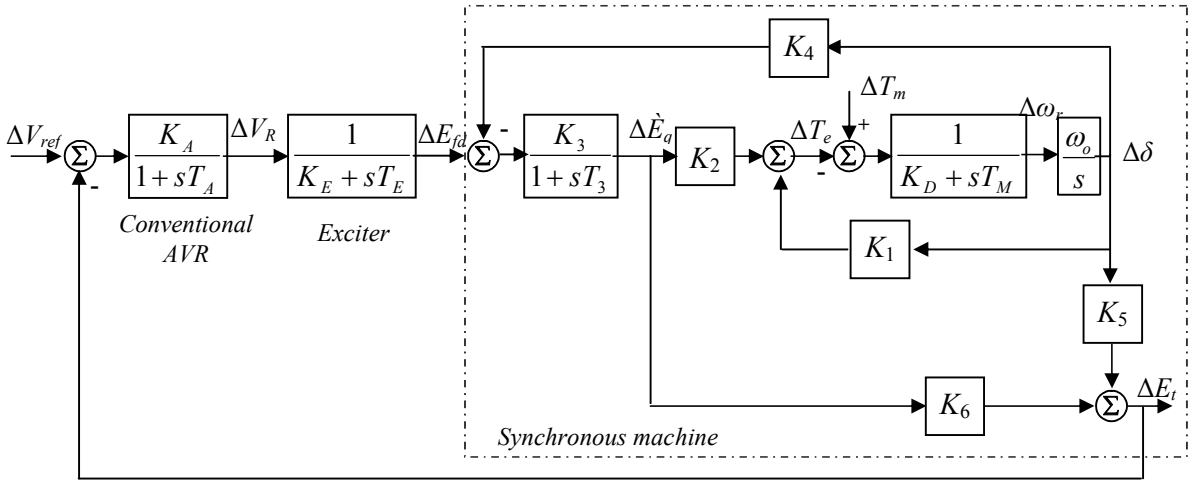

Fig. 8. Detailed Block Diagram of the Linearized Excitation System.

Table 1,
Description of the Excitation System Parameters.

Parameter	Description	Value	Unit
K_D	Damping factor = torque (pu) / speed (pu)	2	pu
T_M	Mechanical starting time	8	sec
K_A	Conventional AVR gain	50	-
T_A	Conventional AVR time constant	0.02	sec
K_E	Exciter gain	0.17	-
T_E	Exciter time constant	0.95	sec
K_1	Synchronous Machine factor	1.0753	
K_2	=	1.2581	
K_3	=	0.3071	
K_4	=	1.7124	
K_5	=	-0.0476	
K_6	=	0.4972	
T_3	Time constant of the field circuit	1.8	Sec
ω_o	Frequency of the system	50	Hz

The detailed block diagram of the excitation control system in figure 8 is redrawn in a compact form in figure 9 fitted with the proposed Digital AVR(DAVR).

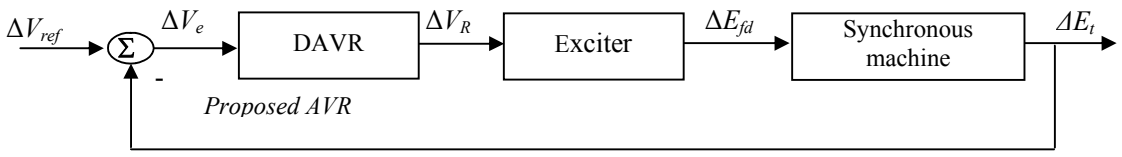

Fig. 9. Block Diagram of the linearized Excitation Control System with the Proposed Digital AVR (DAVR).

This configuration with *Nbar* scaling factor (eq(15)) placed in the feedforward path (see figure 5) will be used to evaluate the proposed DAVR for the excitation control system.

The continuous-time state-space notation of the linearized open-loop system (Exciter + Synchronous machine) can be written as in eq(1), Where u is the control signal and y is the output. Assuming that $\Delta T_m = 0$, then:

$$u = \Delta V_R \qquad x = \begin{bmatrix} \Delta E_{fd} & \Delta \dot{E}_{fd} & \Delta\omega_r & \Delta\delta \end{bmatrix}^T$$

$$y = \begin{bmatrix} \Delta E_t & \Delta\omega_r \end{bmatrix}^T$$

$$A = \begin{bmatrix} -\frac{K_E}{T_E} & 0 & 0 & 0 \\ \frac{K_3}{T_3} & -\frac{1}{T_3} & 0 & -\frac{K_3 K_4}{T_3} \\ 0 & -\frac{K_2}{T_M} & -\frac{K_D}{T_M} & -\frac{K_1}{T_M} \\ 0 & 0 & \omega_o & 0 \end{bmatrix} \quad B = \begin{bmatrix} \frac{1}{T_E} \\ 0 \\ 0 \\ 0 \end{bmatrix}$$

$$C = \begin{bmatrix} 0 & K_6 & 0 & K_5 \\ 0 & 0 & 1 & 0 \end{bmatrix} \qquad D = \begin{bmatrix} 0 \\ 0 \end{bmatrix} \qquad \ldots(17)$$

The above system (eq. (16)) is SIMO (Single Input Multiple Output) and it represents the state-space matrices of the exciter and synchronous generator of figure 7.

4. Results and Simulations

The performance of the excitation system with the conventional AVR is evaluated at different values of the gain (K_A). The MATLAB Control Toolbox is utilized to obtain the results and the simulations. Figures 10 -11 show the terminal voltage (ΔE_t) and the angular speed deviation ($\Delta\omega_r$) due to a step increase in the reference voltage (ΔV_{ref}) by 0.3 pu.

Substituting the typical data of table 1 in eq.(17) and calculating eq.(4) & eq.(5) with sampling time $T_s = 1/100\,\text{sec}$, the discrete-time state-space matrices of the open-loop plant (A_d, B_d) are obtained:

$$A_d = \begin{bmatrix} 0.9982 & 0 & 0 & 0 \\ 0.0055 & 0.9821 & -0.0148 & -0.0094 \\ 0 & -0.0021 & 0.9807 & -0.0018 \\ 0 & 0.0033 & 3.1111 & 0.9972 \end{bmatrix}$$

$$B_d = \begin{bmatrix} 0.0105 \\ 0 \\ 0 \\ 0 \end{bmatrix}$$

$$C_d = C = \begin{bmatrix} 0 & 0.4972 & 0 & -0.0476 \\ 0 & 0 & 1 & 0 \end{bmatrix}$$

$$D_d = D = \begin{bmatrix} 0 \\ 0 \end{bmatrix}$$

With the matrix C given above, Q can be determined by eq (11):

$$Q = \begin{bmatrix} 0 & 0 & 0 & 0 \\ 0 & 0.2472 & 0 & -0.0237 \\ 0 & 0 & 0 & 0 \\ 0 & 0 & -0.0237 & 0.0023 \end{bmatrix}$$

To get a best performance for the terminal voltage (ΔE_t) and of the speed deviation ($\Delta\omega_r$), the elements in main diagonal positions of Q will be used to weight the outputs. Different values of Q & R are selected by trial and error as mentioned in table 2 below.

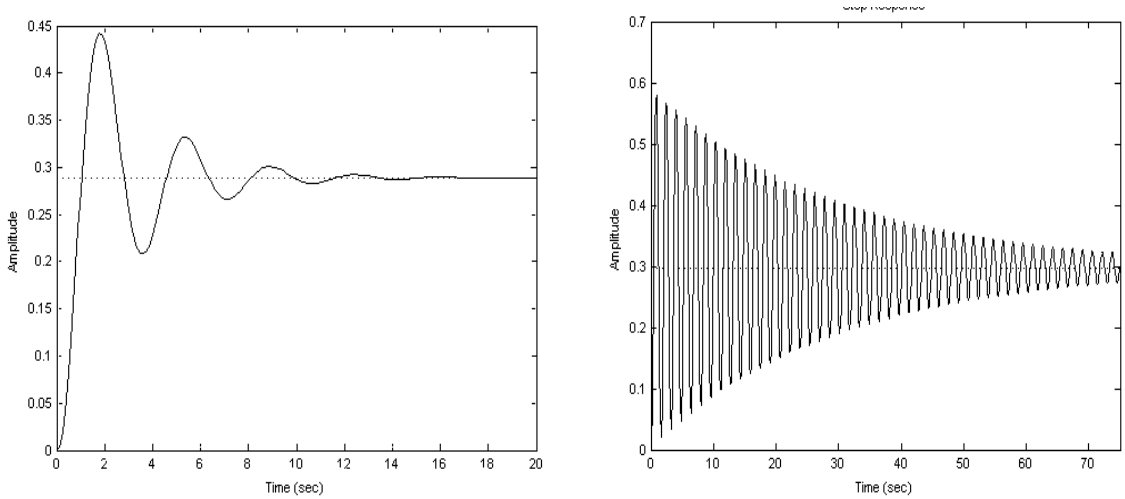

(a) (b)

Fig. 10. Output Response of ΔE_t due to a 0.3 pu Step Increase in ΔV_{ref}, (a) K_A = 10, (b) K_A = 50.

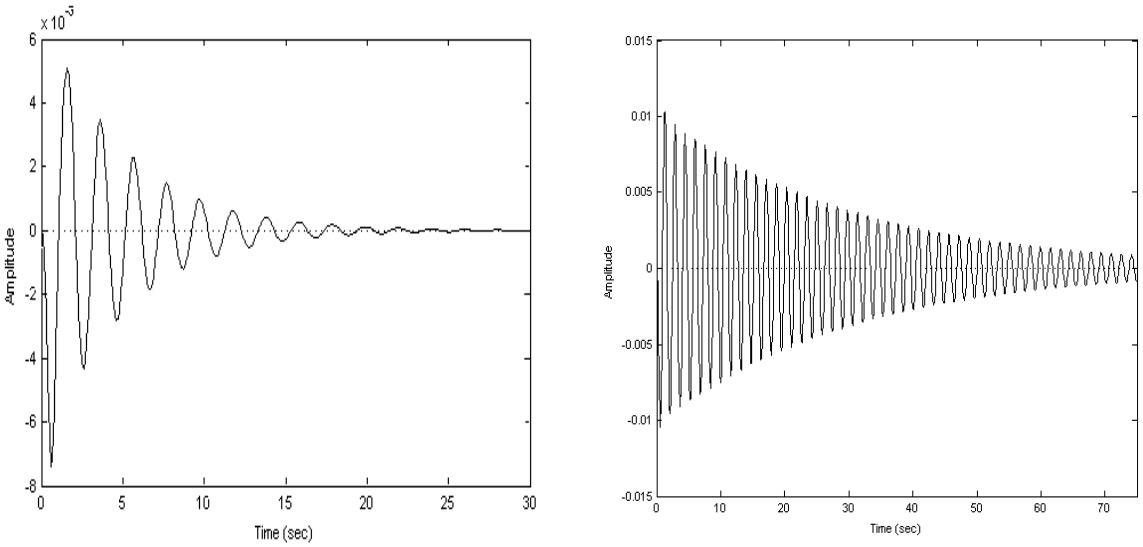

(a) (b)

Fig. 11. Output Response of $\Delta\omega_r$ due to a 0.3 pu Step Increase in ΔV_{ref}, (a) K_A = 30, (b) K_A = 50.

Table 2:
State and control weishting matrices used in the design .

	Q's	*R's*
1	$\begin{bmatrix} 5 & 0 & 0 & 0 \\ 0 & 400 & 0 & -0.0237 \\ 0 & 0 & 100 & 0 \\ 0 & 0 & -0.0237 & 100 \end{bmatrix}$	$[1]$
2	$\begin{bmatrix} 5 & 0 & 0 & 0 \\ 0 & 5 & 0 & -0.0237 \\ 0 & 0 & 10 & 0 \\ 0 & 0 & -0.0237 & 1 \end{bmatrix}$	$[0.1]$
3	$\begin{bmatrix} 1 & 0 & 0 & 0 \\ 0 & 1 & 0 & -0.0237 \\ 0 & 0 & 1 & 0 \\ 0 & 0 & -0.0237 & 0.1 \end{bmatrix}$	$[3]$

With the first raw of Q & R in table 2 , the digital LQR is calculated in (eq. (14)) and found to be:

$$K = [4.6571 \quad 17.4578 \quad -84.9536 \quad 0.6308]$$

With the closed- loop poles calculated as the eignvalues of ($A_d - B_d * K$): 0.9713+j 0.0214, 0.9713-j0.0214, 0.9831+j0.0737, 0.9831-j0.0737, all of the closed-loop eignvalues are inside the unit circle, indicating that the system is asymptotically stable. Time domain performance of the DAVR is depicted in Figure 12, where the terminal voltage (ΔE_t) and the angular speed deviation ($\Delta\omega_r$) are plotted versus time. The design of the considered values of Q and R of table 2 (first raw) and an 0.3 pu step change in the reference voltage (ΔV_{ref}) are applied. It can be seen from the output response of ΔE_t that the settling time is 1 sec with 1.6% overshoot, while the angular speed deviation $\Delta\omega_r$ goes to zero in just 2.35 sec.

The precision of the discrete system mainly depends on the sampling time T_s; figure 13 emphasizes that as the value of T_s gets higher, the output response of the discrete systems gets closer to the analog system's response with $\Delta V_{ref} = 0.5$ pu. Last but not least, the response of the DAVR's with various Q_s and R_s is shown in figure 14 with $\Delta V_{ref} = 0.6$ pu.

Finally, it can be noticed that making values of the Q's diagonal elements small leads to slow response but with less overshoot, while large values introduce large overshoot with swift response. This can be figured out from figure 15. Also, figure 15 describes the relationship between R and the control signal u (ΔV_R), where large value of R decreases ΔV_R and hence the system avoids actuator saturation. On contrast, the control signal ΔV_R goes higher in magnitude and may exceed the allowable limit with small values of R which turns the system into saturation.

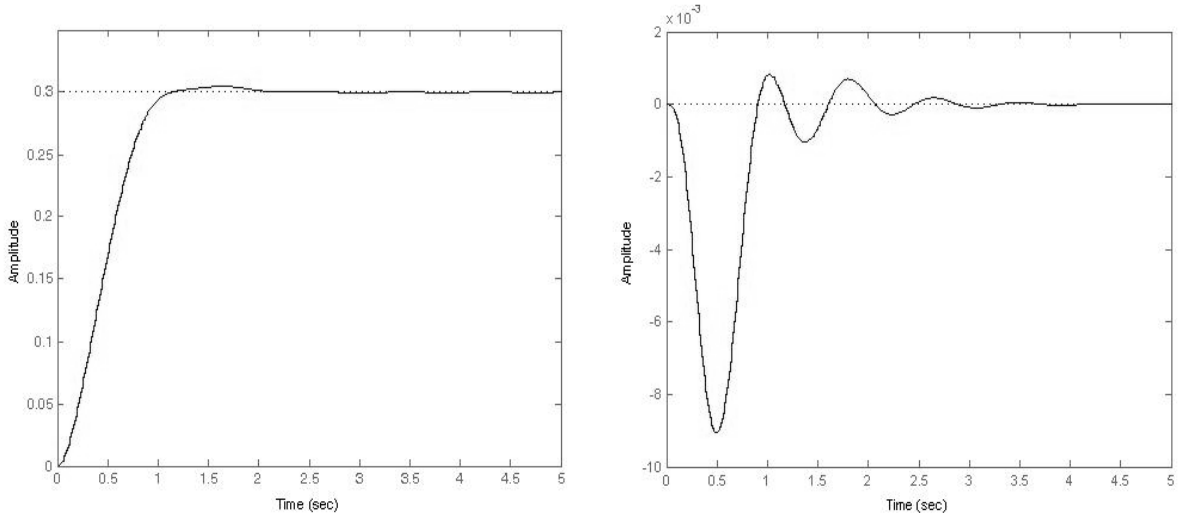

(a) (b)

Fig.12. Output Response of the Excitation Control System with DAVR due to a ΔV_{ref} = 0.3 pu , (a) ΔE_t , (b) $\Delta\omega_r$.

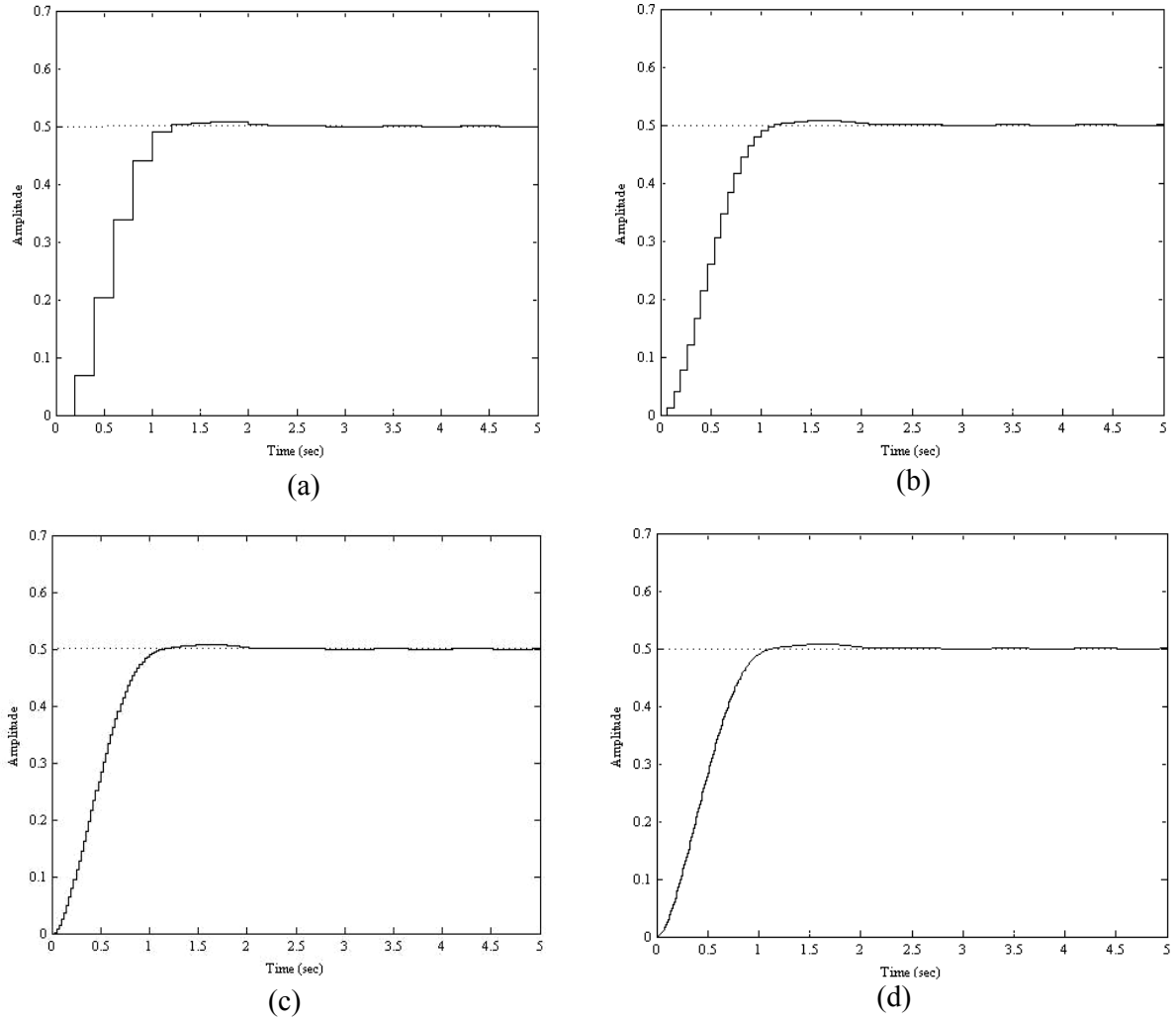

Fig. 13. Output Response of the Excitation Control System (Δ E_t) due to a Δ V_{ref} = 0.5 pu , (a) T_s= 8 sec , (b) T_s=16 sec , (c) T_s= 45 sec, (d) T_s= 85 sec.

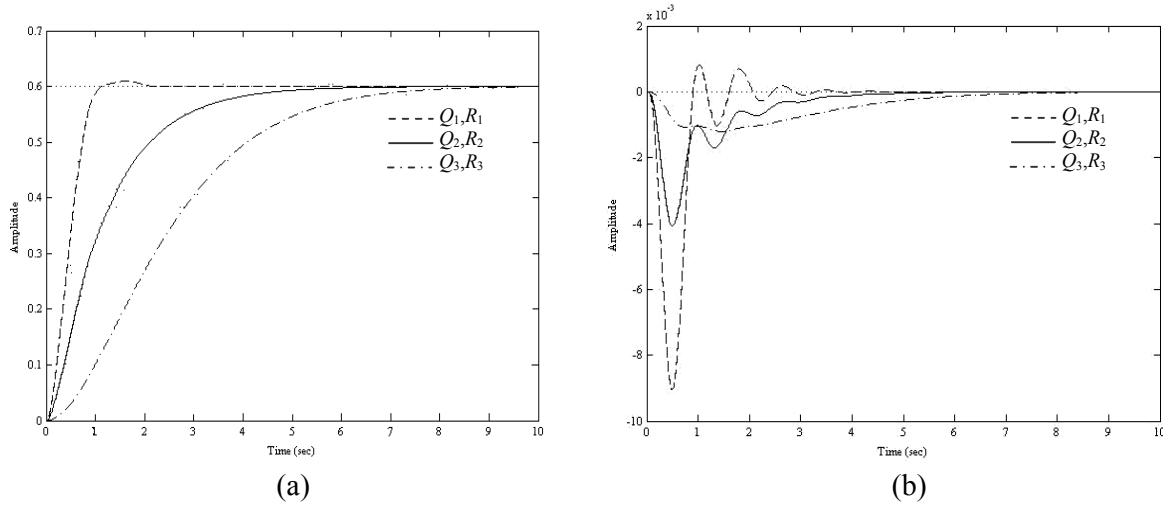

Fig.14. Output Response of the Excitation Control System (Δ E_t) due to a Δ V_{ref} 0.6pu with Different DAVRs, (a) Δ E_t , (b) Δω_r .

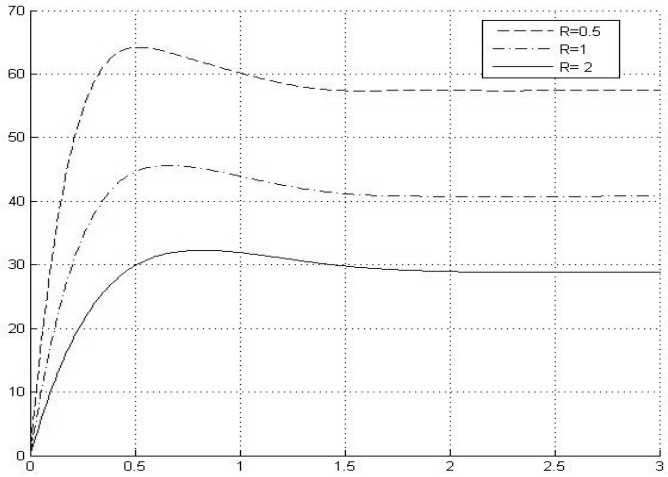

Fig. 15.Output Response of the Control Signal (ΔV_R) for Three Different Control Weighting Matrices (R).

5. Conclusion

In this paper a new optimal digital AVR for the excitation control system is proposed based on the linear quadratic techniques in order to control the terminal voltage ΔE_t of the synchronous generator. The performance of the proposed AVR is evaluated on Single Machine Infinite Bus bar (SMIB) system and compared with the conventional AVR. A set of Q's and R's is chosen and different DAVRs are obtained and tested to restrict the output response of the system within the desired range. Simulations show that in addition to controlling ΔE_t , the proposed DAVR damps well the angular speed deviations $\Delta\omega_r$ in short time.

6. References

[1] Anderson P. M. and Fouad A. A., "Power System Control and Stability", John Wiley and Sons Inc., 2003.

[2] Kundur P., "Power System Stability and Control", McGraw-Hill Inc., 1994.

[3] IEEE Committee Report, "Computer Representation of Excitation Systems", IEEE Transactions on Power Apparatus and Systems, Vol. Pas-87, No. 6, June 1968.

[4] Rangnekar S., "Development of state-Space and Study of Performance Characteristics of Digital Based Excitation Control System ST4B with Single Machine Connected to Infinite Bus", IEEE International Conference on Control Applications, Kohala Coast-Island of Hawai'I, Hawai'I, USA, August 22-27, 1999.

[5] Senjyu T., Yamashita T., Uezato K, and Fujita H., " LMI Approach Based Excitation H∞ Controller Design for Damping of Power System Oscillations and Control of terminal Voltage", IEEE International Conference on Control Applications, 1999.

[6] Venayagamoorthy G. K. and Harley R. G., "A Continually Online Trained Neurocontroller for Excitation and Turbine Control of a Turbogenerator", IEEE Transactions on Energy Conversion, Vol. 16, No. 3, September 2001.

[7] Venayagamoorthy G. K. and Harley R. G., " Two Separate Continually Online-Trained Neurocontrollers for Excitation and Turbine Control of a Turbogenerator", IEEE Transactions on Industry Applications, Vol. 38, No. 3, May/June 2002.

[8] Mitra, P., Chowdhury S.P., Pal S.K., and Crossley P.A., "Intelligent AVR and PSS with Adaptive hybrid learning algorithm", IEEE Power and Energy Society General Meeting - Conversion and Delivery of Electrical Energy in the 21st Century, pages:1-7, 2008.

[9] Fusco G. and Russo M., "A Adaptive Voltage Regulator Design for Synchronous Generator", IEEE Transactions on Energy Conversion, Vol. 23 , Issue 3, pages: 946-956, 2008.

[10] Mohammadi, S. M. A., Gharaveisi A. A., Mashinchi M., and Rafiei S. M. R., "New Evolutionary Methods For Optimal Design Of PID Controllers for AVR System ",

IEEE Conference on Power Tech, pages 1-8, Bucharest, Jun 28-Jul 2, 2009.

[11] Yoshimura S., Iki H., Uriu Y., Anai H., and Hyodo N., "Generator excitation control using a parameter space design method ",43rd international universities power engineering conference, pages 1-4,Padova, Italy,1-4 September, 2008.

[12] Dysko A., Leithead W. E., O'Reilly J., "Enhanced Power System Stability by Coordinated PSS Design " IEEE Transactions on Power Systems, pages 413-422, 2010.

[13] Ogata K., "Modern Control Engineering", Prentice-Hall International, Inc, 1973.

[14] "Control Tutorial for MATLAB and Simulink", a website: http://www.engin.umich.edu/class/ctms/index.htm

[15] Franklin G. F., Powell J. D., and Workman M. L., "Digital Control of Dynamic Systems", Adison-Wesley, 3rd Edition, 1998.

[16] Fadali M. S., "Digital Control Engineering: Analysis and Design", Elsevier Inc, 2009.

[17] Ogata K., "Modern Control Engineering", 4th edition, Prentice-Hall International, Inc, 2002.

[18] Moudgalya K. M., "Digital Control", John Wiley & Sons, Ltd, 2007.

[19] "Control System Toolbox", MATLAB, The MathWorks, Inc, 2009.

[20] Dutton K., Thompson S., and Barraclough B., "The Art of Control Engineering ", Adison-Wesley,1997.

[21] Law B. E., "Simulation of the transient response of synchronous machines", B.Sc. thesis, the university of Queensland, School of Information Technology and Electrical Engineering, October, 2001.

[22] Chen S. and Malik O. P., "Power System Stabilizer Design using μ Synthesis", IEEE Transactions on Energy Conversion, Vol. 10, No. 1, March 1995.

[23] Franklin G. F., Powell J. D., and Workman M. L., "A Robust H∞ Synthesis Controller for Power System Stabilization",, ASCE Journal, Volume (5), Issue (II), June, 2005.

[24] IEEE Power Engineering Society, "IEEE Recommended Practice for Excitation System Models for Power System Stability Studies", IEEE Inc., 21 April 2006.

تصميم منظم فولتية متناوبة رقمي للمولد التزامني باستخدام طريقة التربيع الخطي

إبراهيم قاسم إبراهيم
قسم هندسة الحاسبات/ كلية الهندسة/ جامعة بغداد
البريد الالكتروني: ibraheem151@gmail.com

الخلاصة

في هذا البحث هيكلية جديدة لمنظم الفولتية المتناوب للمثير الخاص بالمولد التزامني تم اقتراحه بالاعتماد على طريقة المنظم التربيعي الخطي الرقمي. مع مصفوفتي تعيير هما R والطريقة تعطي منظم تقاضلي الذي يستخدم لتوليد قانون السيطرة الاسترجاعي. هاتان المصفوفتان تدعيان مصفوفتي الحالة والسيطرة ويستخدمان للموازنة بين الاهمية النسبية للادخال وحالات المنظومة في دالة الكلفة التي تُفاضَل. منظومة قدرة نوعية متكونة من مولدة واحدةمربوطة الى خط نقل مع كلاً من الطريقتين التقليدية والمقترحة (نظم الفولتية المتناوب الرقمي) قد تمت محاكاتها .نتائج التقييم اظهرت ان الطريقة المقترحة تم(نظم الفولتية المتناوب الرقمي)يخمد تذبذبات الفولتية الطرفية بطريقة جيدة ويقدم استجابة اسرع من منظم الفولتية التقليدي.